

On the half-metallicity of Co₂FeSi Heusler alloy: an experimental and *ab initio* study

L. Makinistian,^{1,2} Muhammad M. Faiz,³ Raghava P. Panguluri,³ B. Balke,⁴
S. Wurmehl,⁴ C. Felser,⁴ E. A. Albanesi,^{1,2} A. G. Petukhov,⁵ and B. Nadgorny³

¹*INTEC-CONICET, Güemes 3450, 3000 Santa Fe, Argentina*

²*Facultad de Ingeniería, Universidad Nacional de Entre Ríos, 3101 Oro Verde, Argentina*

³*Department of Physics and Astronomy, Wayne State University, Detroit MI, 48201*

⁴*Institut für Anorganische Chemie und Analytische Chemie,*

Johannes Gutenberg-Universität, D-55099 Mainz, Germany

⁵*South Dakota School of Mines, Department of Physics, Rapid City, South Dakota 57701-3995*

Co₂FeSi, a Heusler alloy with the highest magnetic moment per unit cell and the highest Curie temperature, has largely been described theoretically as a half-metal. This conclusion, however, disagrees with Point Contact Andreev Reflection (PCAR) spectroscopy measurements, which give much lower values of spin polarization, P . Here, we present the spin polarization measurements of Co₂FeSi by the PCAR technique, along with a thorough computational exploration, within the DFT and a GGA+U approach, of the Coulomb exchange U -parameters for Co and Fe atoms, taking into account spin-orbit coupling. We find that the orbital contribution (m_o) to the total magnetic moment (m_T) is significant, since it is at least 3 times greater than the experimental uncertainty of m_T . Account of m_o radically affects the acceptable values of U . Specifically, we find no values of U that would simultaneously satisfy the experimental values of the magnetic moment and result in the half-metallicity of Co₂FeSi. On the other hand, the ranges of U that we report as acceptable are compatible with spin polarization measurements (ours and the ones found in the literature), which all are within approximately 40-60% range. Thus, based on reconciling experimental and computational results, we conclude that: a) spin-orbit coupling cannot be neglected in calculating Co₂FeSi magnetic properties, and b) Co₂FeSi Heusler alloy is not half-metallic. We believe that our approach can be applied to other Heusler alloys such as Co₂FeAl.

PACS numbers: 71.20.-b, 71.20.Be, 75.70.Cn

While Heusler compounds have been known for more than a hundred years¹, they drew a remarkable amount of attention²⁻⁶ ever since the prediction by de Groot *et al.*^{7,8} in the early 1980's that some of these alloys would have a metallic band structure for the majority spin channel and a semiconducting band structure for the minority one, resulting in 100% spin-polarization (P) at the Fermi level. Such *half-metallic* (HM) materials, with high values of P and Curie temperature (T_c), are excellent candidates for spintronic applications^{9,10} (e.g., magnetic random access memories (MRAM)¹¹ utilizing the giant magneto-resistance spin-valve effect¹² in magnetic tunnel junctions¹³). Specifically for Co₂FeSi, high and low temperature magnetometry experiments¹⁴ showed that it is a Heusler compound with the highest magnetic moment ($(5.97 \pm 0.05)\mu_B$ per unit cell, at 5 K) and the highest T_c (1100 K) among other Heusler alloys.

Detailed computational studies have indicated that an orbital-dependent potential accounting for a moderate Coulomb-exchange interaction must be included in self-consistent calculations to simultaneously replicate both the experimental equilibrium lattice parameter (5.64 Å) and the measured magnetic moment of Co₂FeSi alloy.^{14,15} These studies have also revealed that a total spin magnetic moment $\sim 6\mu_B$ can be obtained only for the effective Coulomb-exchange interaction parameters¹⁶ ($U_{eff} = U - J$) falling within the ranges of 2.5-5 eV and 2.4-4.8 eV for the d-orbitals of Co and Fe atoms, respectively. Even though Co₂FeSi alloy appears to be half-metallic only theoretically and only

under stringent conditions on U_{eff} , it has been extensively referenced in the literature as such.¹⁷⁻²² This prediction, however, is at odds with several experimental measurements based on Point Contact Andreev Reflection (PCAR) spectroscopy^{17,22,23}, which yield values of $P \sim 50\%$, far lower than 100%.

The goal of this Rapid Communication is to reconcile the results of computational predictions with experimental measurements for Co₂FeSi. First, we present the results of our own PCAR measurements of P and compare them with those available in the literature. Second, we perform a thorough computational exploration of the Coulomb exchange U -parameter space for the 3d-orbitals of Co and Fe atoms in Co₂FeSi, seeking the domain of parameters allowing to replicate the experimental measurements.

The samples were prepared by arc melting of stoichiometric amounts of the constituents in an argon atmosphere at 10^{-4} mbar. The polycrystalline ingots were then annealed in an evacuated quartz tube at 1273 K for 21 days. This procedure resulted in samples exhibiting the Heusler type L2₁ structure, which was verified by X-ray powder diffraction (XRD) using excitation by Mo K_{α1} radiation. Flat disks were cut from the ingots and polished for spectroscopic investigations of bulk samples. X-ray photo emission (ESCA) was used to verify the composition and to check the cleanliness of the samples. After removal of the native oxide from the polished surfaces by Ar⁺ ion bombardment, no impurities were

detected with ESCA.

For the PCAR measurements, niobium superconducting tips are fabricated by electrochemical etching of 250 μm thick niobium wire in a solution of HNO_3 , HF , and CH_3COOH , with a mixing ratio of 5:4:1 by volume. The wire was kept at a positive potential with respect to the graphite counter electrode. The applied voltage was optimized at $\sim 8\text{--}10$ V for the output current of $\sim 800\text{--}0$ mA to get a sharp tip, see Fig. 1a) and b). Just before the measurements the tip was briefly dipped into the HF solution. A freshly etched superconducting Nb tip (bulk $T_C \sim 9.3$ K) was then mounted onto a shaft connected to a differential type screw that could be driven manually by 10 μm per revolution. For the low temperature measurements both the tip and the sample were immersed into a liquid He bath. The current-voltage ($I\text{--}V$) measurements were taken using a four-probe technique, with the differential conductance dI/dV obtained by standard ac lock-in detection at a frequency of 2 kHz within the temperature range 1.2–4.2 K. Typical results for normalized conductance $G(V)/G_n$ as a function of voltage V are shown in Fig. 1c). At least 15 different junctions with the contact resistance $1\ \Omega \leq R_C \leq 100\ \Omega$ were measured and analyzed. To extract the values of spin polarization, P , the conductance curves for each junction were fitted with the modified²⁴ BTK model²⁵, using the value of Nb superconducting gap, $\Delta = 1.5$ meV. As the values of P were found practically independent of the interface transparency Z , the values for individual contacts were averaged out. The red circles in Fig. 1c) represent the experimental data and the dashed black line is the fit. We find that the average value of spin polarization $\langle P \rangle = 48 \pm 3\%$, Table I, shows that our results are in good agreement with the other PCAR measurements available in the literature.

TABLE I: Experimental spin polarizations of Co_2FeSi by the PCAR technique.

P(%)	PCAR on Co_2FeSi	Ref.
48 ± 3	bulk @1.2 K	this work
49 ± 2	thin films on MgO (001) @4.2 K	17
57 ± 1	bulk @4.2 K	23
59 ± 2	thin films on n-Ge(111) @4.2 K	22

In order to proceed, we need to calculate the spin polarization, P_n , that can be defined by^{26–28}:

$$P_n = \frac{\langle N_\uparrow v_\uparrow^n \rangle - \langle N_\downarrow v_\downarrow^n \rangle}{\langle N_\uparrow v_\uparrow^n \rangle + \langle N_\downarrow v_\downarrow^n \rangle} \times 100 \quad (1)$$

where the averages are taken upon all the sheets of the Fermi surface, and the exponent n depends on the details of the experimental technique. For spin-resolved photoemission $n=0$ (P_0 is the “static” or “intrinsic” spin polarization); $n=1$ corresponds to experiments in the ballistic transport regime, whereas $n=2$ describes experiments dominated by diffusive transport. Ideally the PCAR experiments are done in the ballistic (Sharvin) regime, but

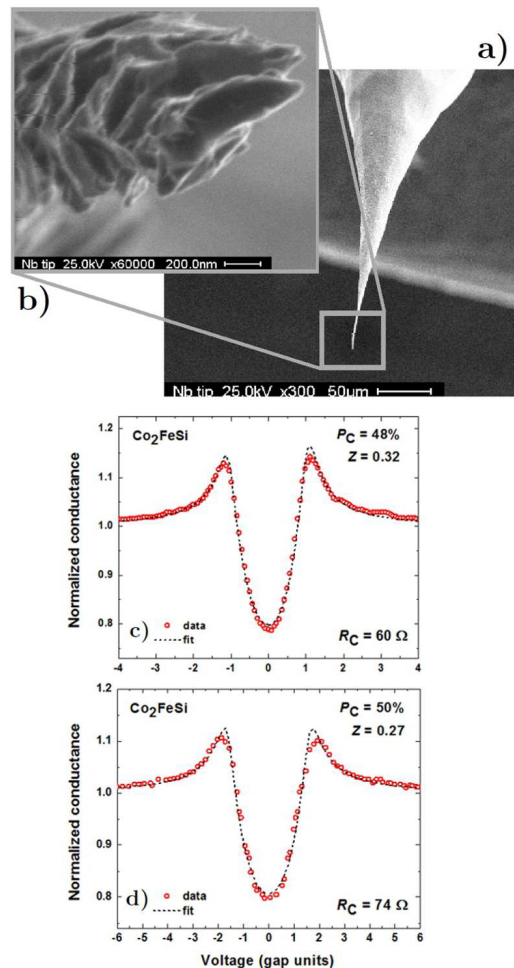


FIG. 1: (Color online) Superconducting Nb tip: a) shows a scanning electron micrograph of a tip ($\times 300$), and b) shows just the apex of a tip from a different angle and a greater amplification ($\times 60000$). c-d) Optimum normalized conductance curves for Nb/ Co_2FeSi contacts as a function of voltage with Nb superconducting gap, $\Delta = 1.5$ meV and $T = 1.2$ K. The red circles represent the experimental data and the dashed black line is the fit.

if the mean free path is smaller than the minimum size of the contact, they can only be performed in the diffusive regime.^{29,30} It is clear from Eq. (1) that while P_0 can be directly calculated from the spin polarized density of states (DOS), P_1 and P_2 , in addition to the DOS, also require the respective Fermi velocities. Following the approach of Scheidemantel *et al.*³¹, we calculated the Fermi velocity directly from the matrix elements of the momentum operator (instead of differentiating Bloch energies $E_{i,\vec{k}}$ with respect to \vec{k}) according to:

$$\vec{v}_{i,\vec{k}} = \frac{1}{m} \langle \psi_{i,\vec{k}} | \hat{\vec{p}} | \psi_{i,\vec{k}} \rangle \quad (2)$$

where i is the band index. These matrix elements can be readily generated using the optical package of the full potential linearized augmented plane waves (FP-

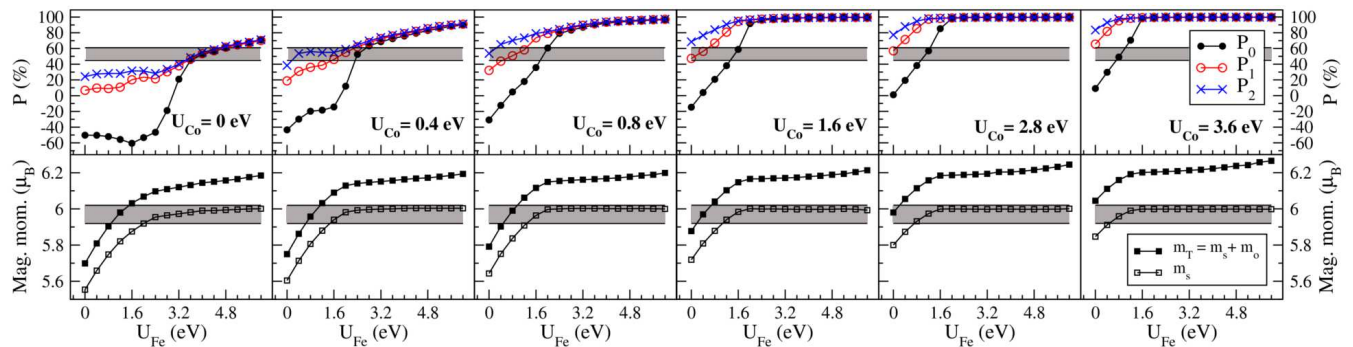


FIG. 2: (Color online) Spin polarizations (P_0 , P_1 and P_2 , see text for details), and spin (m_s) and total (spin plus orbital: $m_T = m_s + m_o$) magnetic moment for selected values of U_{Co} (from left to right: 0, 0.4, 0.8, 1.6, 2.8, 3.6 eV) and U_{Fe} in the range 0-6 eV. The gray shaded areas mark the experimental ranges for total magnetic moment¹⁴: $m_T = 5.97 \pm 0.05$ and the spin polarization (see Table I): $45 < P < 61$.

LAPW)^{32–37} WIEN2k code³⁸, and further used as an input in Eq. (1) to calculate P_1 and P_2 . We tested this procedure for pure bcc Fe and fcc Ni. As we can see from Table II our results are in satisfactory agreement with other calculations and experimental data available in the literature.

TABLE II: Our calculated spin polarizations (in %) for bcc Fe and fcc Ni, against others' calculations (figs. 2-3 in ^aRef.³⁰, ^bRef.³⁹) and experiments (^bRef.³⁹, ^cRef.²⁹).

	bcc Fe			fcc Ni		
	Ours	Others	Exp.	Ours	Others	Exp.
P_0	51	58 ^a , 59 ^b	-	-80	-81 ^a	-
P_1	39	39 ^a , 33 ^b	-	-45	-48 ^a	-
P_2	37	33 ^a , 21 ^b	-	5	2 ^a	-
P_{exp}	-	-	44 ± 3^b , 40-48 ^c	-	-	40-47.5 ^c

We carried out all our calculations with the WIEN2K code, using the generalized gradient approximation (GGA) in the formal parameterization scheme of Perdew-Burke-Ernzerhof (PBE)⁴⁰ and the experimental lattice parameter of 5.64 Å for the cubic Co₂FeSi (crystallographic details of its structure can be found in Ref.⁴¹). Muffin tin radii (R_{MT}) of 2.32, 2.32, and 2.18 atomic units were used for the Co, Fe, and Si atoms, respectively. The $R_{MT}^* \cdot K_{max}$ product, where R_{MT}^* is the smallest of all muffin tin radii, and K_{max} is the plane wave cut-off, was set equal to 7 (implying a plane wave expansion cut-off of ~ 9.10 Ry), and the energy threshold between core and valence states used was of -6.0 Ry. Integration in the irreducible Brillouin zone was carried out over 641 k-points and convergence was set to simultaneously be better than 10^{-4} (Ry) for the total energy and 10^{-3} (au) for the total electronic charge. Spin-orbit coupling was included in all calculations in order to obtain not only the total spin, but also the total orbital moment. Within the LDA(GGA)+U scheme¹⁶ we have modified the 3d orbitals of Co and Fe atoms, and explored a square mesh of 16×16 points in the U_{Co} - U_{Fe} space (resulting in a total

of 256 self-consistent calculations), with $0 \leq U_{Co} \leq 6$ eV and $0 \leq U_{Fe} \leq 6$ eV. Since it has been shown⁴² that the choice of different “flavors” of the double counting correction of the +U method can be critical, we tested two of them: one, the so-called “SIC” (self-interaction correction), introduced by Anisimov et al.^{16,43}, and the “AMF” (around mean field), introduced by Czyżyk and Sawatzk⁴⁴. The latter yielded the total magnetic moments (spin plus orbital terms) lower than the lowest bound of the experiments ($5.92 \mu_B$)¹⁴ up to $U \sim 5$ eV, so we found it inadequate for modeling Co₂FeSi. Thus, all the results reported here were obtained using the SIC flavor of the method.

Representative sampling of our results is shown in Fig. 2, where, the total spin moment (m_s), the total magnetic moment (m_T , i.e., total spin (m_s) plus total orbital (m_o) moment), and the spin polarizations P_0 , P_1 , P_2 are presented as a function of U_{Co} and U_{Fe} . It is clear that for a system where spin-orbit coupling is important, such as the case for Co₂FeSi, the spin-orbit interaction induces a strong orbital component in the m_T , which turns out to be significant and cannot be neglected: it shifts to lower energies, and simultaneously narrows down, the range of U_{Fe} that yields a total magnetization within the experimental margin of error, $m_T = 5.97 \pm 0.05$ ¹⁴ (see the gray shaded area in the bottom panels of Fig. 2). One can also see from Fig. 2 that for $U_{Co} \geq 3.6$ eV none of the U_{Fe} -values would yield the value of m_T within the experimental range. The total spin moment is also shown in all of the bottom panels (it is fixed at $6 \mu_B$ beyond a certain value of U_{Fe}). The analysis of all our calculations allows us to produce Figs. 3a) and b), that show the values of the U-parameter (areas within the closed loops in the figure) for which the calculated total magnetic moment and spin polarizations (P_0 , P_1 , or P_2) are within the experimental range. Finally, Fig. 3d) shows the values of U for which our calculations simultaneously agree with the results of both: magnetometry and PCAR spectroscopy (the latter is taken over the entire range, $45\% < P < 61\%$, defined by our measurements and oth-

ers, see Table I). Except for the lower area ($U \sim 0.4$ eV, which corresponds to P_2), all other values correspond to P_1 , i.e., the expected ballistic transport between the superconducting tip and the sample in the PCAR experiments with Co_2FeSi . Thus, in view of our findings, the results of magnetometry measurements indicate that Co_2FeSi is actually not a half-metal, and the determination of P using PCAR spectroscopy is fully compatible with this prediction.

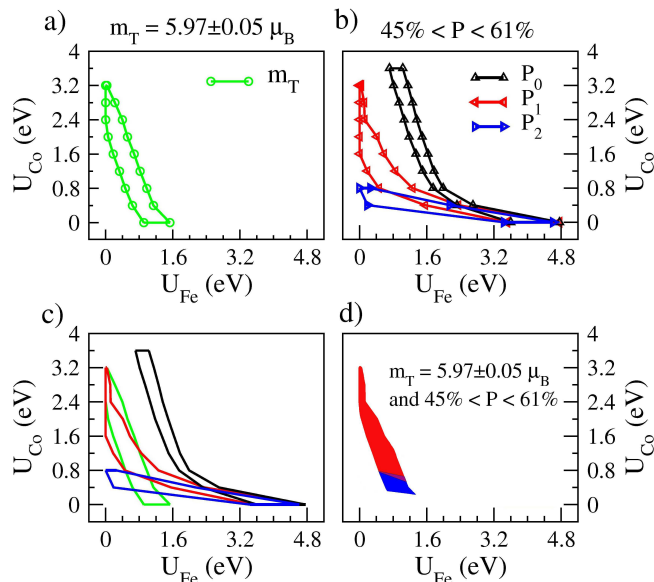


FIG. 3: (Color online) The area within the closed loops correspond to values of U for which a) the calculated total magnetic moment, m_T , agrees with experiment; b) the spin polarizations (P_0 , P_1 , or P_2) are within the experimental PCAR values. c) The four loops of a) and b) are superimposed (omitting the symbols) to aid the eye. d) Intersection of the areas of a) and b), i.e., the values of U for which both calculated m_T and P values fall within experimental values.

Chalsani *et al.*⁴⁵ mentioned that the results of the PCAR technique can be affected by a number of factors, such as the geometry of the contact and interactions between the sample and the tip through surface states; however, *ab initio* calculations by Khosravizadeh

*et al.*⁴⁶ showed that the surface of Co_2FeSi is also non half-metallic, and the loss half-metallicity of Co_2FeSi , which we have found, cannot be attributed to the surface effects. Moreover, our results for a perfect bulk material would persist, regardless of whether or not anti-site defects, finite temperature⁴⁷, and crystallographic disorder^{48,49}, could induce additional loss of half-metallicity by the appearance of spin states in the minority spin channel. The orbital moments we calculated in Co_2FeSi depend on the U -parameter, ranging from $0.145 \mu_B$ for $U_{\text{Co}} = U_{\text{Fe}} = 0$, to $0.482 \mu_B$ for $U_{\text{Co}} = U_{\text{Fe}} = 6$ eV. One key idea presented here is that even the lowest orbital moment obtained ($m_o = 0.145 \mu_B$) is almost three times greater than the experimental uncertainty ($0.05 \mu_B$) in the magnetometry measurements of the total magnetic moment per formula unit¹⁴ ($m_T = 5.97 \pm 0.05 \mu_B$), as Fig. 2 clearly demonstrates. In addition, the total spin moment as is shown in Fig. 2 (in all the bottom panels) is fixed at $6 \mu_B$ beyond a certain value of U_{Fe} . It is also seen that for $U_{\text{Co}} = 3.6$ eV there is no U_{Fe} value that would yield an m_T within the experimental range. Our calculations of m_o , are also supported by the systematic study by Galanakis⁵⁰, performed on nine full-Heuslers alloys, and while the author does not study Co_2FeSi , he presents the results on similar compounds, Co_2FeAl and Co_2MnSn , citing for the former the greatest total orbital moment calculated in that work to be $0.149 \mu_B$, which is in excellent agreement with our $0.145 \mu_B$ value.

In summary, our calculations provide a strong evidence that the orbital component of the total magnetic moment in Co_2FeSi cannot be neglected. By taking it into account we identify the ranges of the U -parameters compatible with both the magnetometry and PCAR (ours and others) measurements. Based on the range of the U -parameters, we conclude that Co_2FeSi is not a half-metal. We believe that our approach will be applicable to other compounds similar to Co_2FeSi , such as Co_2FeAl and Co_2MnSn .

This work was supported by DOE Grant No. DE-SC0004890 at SDSM&T, the Consejo Nacional de Investigaciones Científicas y Técnicas (CONICET), and the Universidad Nacional de Entre Ríos (UNER), Argentina.

¹ F. Heusler, Verh. Deutsche Phys. Ges. **5**, 559 (1903).

² J. Kübler, A. R. Williams, and C. B. Sommers, Phys. Rev. B **28**, 1745 (1983).

³ I. Galanakis, P. H. Dederichs, and N. Papanikolaou, Phys. Rev. B **66**, 174429 (2002).

⁴ G. H. Fecher, H. C. Kandpal, S. Wurmehl, C. Felser, and G. Schönhense, J. Appl. Phys. **99**, 08J106 (2006).

⁵ Y. Miura, K. Nagao, and M. Shirai, Phys. Rev. B **69**, 144413 (2004).

⁶ K. Hamaya, N. Hashimoto, S. Oki, S. Yamada, M. Miyao, and T. Kimura, PRB **85**, 100404(R) (2012).

⁷ R. A. de Groot, F. M. Mueller, P. G. vanEngen, and

K. H. J. Buschow, Phys. Rev. Lett. **50**, 2024 (1983).

⁸ R. A. de Groot, F. M. Mueller, P. G. van Engen, and K. H. J. Buschow, J. Appl. Phys. **55**, 2151 (1984).

⁹ I. Žutić, J. Fabian, and S. Das Sarma, Rev. Mod. Phys. **76**, 323 (2004).

¹⁰ C. Felser, G. H. Fecher, and B. Balke, Angew. Chem. (int. ed.) **46**, 668 (2007).

¹¹ S. S. P. Parkin *et al.*, J. Appl. Phys. **85**, 5828 (1999).

¹² B. Dieny, V. S. Speriosu, S. S. P. Parkin, B. A. Gurney, D. R. Wilhoit, and D. Mauri, Phys. Rev. B **43**, 1297 (1991).

¹³ J. S. Moodera, L. R. Kinder, T. M. Wong, and R. Meserve, Phys. Rev. Lett. **74**, 3273 (1995).

- ¹⁴ S. Wurmehl, G. H. Fecher, H. C. Kandpal, V. Ksenofontov, C. Felser, H. J. Lin, and J. Morais, *Phys. Rev. B* **72**, 184434 (2005).
- ¹⁵ H. C. Kandpal, G. H. Fecher, C. Felser, and G. Schönhense, *Phys. Rev. B* **73**, 094422 (2006).
- ¹⁶ V. I. Anisimov, F. Aryasetiawan, and A. I. Lichtenstein, *J. Phys.: Condens. Matter* **9**, 767 (1997).
- ¹⁷ Z. Gercsi, A. Rajanikanth, Y. K. Takahashi, K. Honob, M. Kikuchi, N. Tezuka, and K. Inomata, *APL* **89**, 082512 (2006).
- ¹⁸ Z. Gercsi and K. Hono, *J. Phys.: Condens. Matter* **19**, 326216 (2007).
- ¹⁹ Y. Takamura, R. Nakane, H. Munekata, and S. Sugahara, *JAP* **103**, 07D719 (2008).
- ²⁰ S. Yamada, K. Hamaya, K. Yamamoto, T. Murakami, K. Mibu, and M. Miyao, *APL* **96**, 082511 (2010).
- ²¹ K. Kasahara, K. Yamamoto, S. Yamada, T. Murakami, K. Hamaya, K. Mibu, and M. Miyao, *JAP* **107**, 09B105 (2010).
- ²² S. Yamada, K. Hamaya, T. Murakami, B. Varaprasad, Y. K. Takahashi, A. Rajanikanth, K. Hono, and M. Miyao, *JAP* **109**, 07B113 (2011).
- ²³ S. V. Karthik, A. Rajanikanth, T. M. Nakatani, Z. Gercsi, Y. K. T. T. Furubayashi, K. Inomata, and K. Hono, *JAP* **102**, 043903 (2007).
- ²⁴ I. Mazin, A. Golubov, and B. Nadgorny, *Journ Appl. Phys.* **89**, 7576 (2001).
- ²⁵ G. E. Blonder, M. Tinkham, and T. M. Klapwijk, *Phys. Rev. B* **25**, 4515 (1982).
- ²⁶ I. I. Mazin, *PRL* **83**, 1427 (1999).
- ²⁷ B. Nadgorny, I. I. Mazin, M. Osofsky, R. J. Soulen, Jr., P. Broussard, R. M. Stroud, D. J. Singh, V. G. Harris, A. Arsenov, and Y. Mukovskii, *Phys. Rev. B* **63**, 184433 (2001).
- ²⁸ G. Sheet, H. Rosner, S. Wirth, A. Leithe-Jasper, W. Schnelle, U. Burkhardt, J. A. Mydosh, P. Raychaudhuri, and Yu Grin, *PRB* **72**, 180407 (2005).
- ²⁹ R. Soulen, Jr., J. M. Byers, M. S. Osofsky, B. Nadgorny, T. Ambrose, S. F. Cheng, P. R. Broussard, C. T. Tanaka, J. Nowak, J. S. Moodera, et al., *Science* **282**, 85 (1998).
- ³⁰ M. S. Bahrany, P. Murugan, G. P. Das, and Y. Kawazoe, *PRB* **75**, 054404 (2007).
- ³¹ T. J. Scheidemantel, C. Ambrosch-Draxl, T. Thonhauser, J. V. Badding, and J. O. Sofo, *PRB* **68**, 125210 (2003).
- ³² D. Koelling and G. Arbman, *J. Phys. F: Met. Phys.* **5**, 2041 (1975).
- ³³ O. K. Andersen, *Phys. Rev. B* **12**, 3060 (1975).
- ³⁴ O. Jepsen, J. Madsen, and O. K. Andersen, *Phys. Rev. B* **26**, 2790 (1982).
- ³⁵ M. Weinert, E. Wimmer, and A. J. Freeman, *Phys. Rev. B* **26**, 4571 (1982).
- ³⁶ H. J. F. Jansen and A. J. Freeman, *Phys. Rev. B* **30**, 561 (1984).
- ³⁷ L. F. Mattheiss and D. R. Hamann, *Phys. Rev. B* **33**, 823 (1986).
- ³⁸ K. Schwarz, P. Blaha, and G. K. H. Madsen, *Comput. Phys. Commun.* **147**, 71 (2002).
- ³⁹ B. Nadgorny, R. J. Soulen, Jr., M. S. Osofsky, I. I. Mazin, G. Laprade, R. J. M. vandeVeerdonk, A. A. Smits, S. F. Cheng, E. F. Skelton, and S. B. Qadri, *PRB* **61**, R3788 (2000).
- ⁴⁰ J. P. Perdew, K. Burke, and M. Ernzerhof, *Phys. Rev. Lett.* **77**, 3865 (1996).
- ⁴¹ Aniruddha Deb, M. Itou, Y. Sakurai, N. Hiraoka, and N. Sakai, *Phys. Rev. B* **63**, 064409 (2001).
- ⁴² A. G. Petukhov, I. I. Mazin, L. Chioncel, and A. I. Lichtenstein, *PRB* **67**, 153106 (2003).
- ⁴³ V. I. Anisimov, I. V. Solovyev, M. A. Korotin, M. T. Czyżyk, and G. A. Sawatzky, *PRB* **48**, 16929 (1993).
- ⁴⁴ M. T. Czyżyk and G. A. Sawatzky, *PRB* **49**, 14211 (1994).
- ⁴⁵ P. Chalsani, S. K. Upadhyay, O. Ozatay, and R. A. Buhrman, *PRB* **75**, 094417 (2007).
- ⁴⁶ S. Khosravizadeh, S. J. Hashemifar, and H. Akbarzadeh, *PRB* **79**, 235203 (2009).
- ⁴⁷ J. J. Attema, C. Fang, L. Chioncel, G. A. de Wijs, A. I. Lichtenstein, and R. A. de Groot, *J. of Phys.: Condens. Matter* **16**, S5517 (2004).
- ⁴⁸ D. Orgassa, H. Fujiwara, T. C. Schulthess, and W. H. Butler, *PRB* **60**, 13237 (1999).
- ⁴⁹ R. P. Panguluri, S. Xu, Y. Moritomo, I. V. Solovyev, and B. Nadgorny, *APL* **94**, 012501 (2009).
- ⁵⁰ I. Galanakis, *PRB* **71**, 012413 (2005).